

Forces of Interaction between Poly(2-vinylpyridine) Brushes As Measured by Optical Tweezers

Mahdy M. Elmahdy,^{†,§} Alla Synytska,[‡] Astrid Drechsler,[‡] Christof Gutsche,[†] Petra Uhlmann,[‡] Manfred Stamm,[‡] and Friedrich Kremer^{*,†}

[†]Institute of Experimental Physics I, Leipzig University, Linnéstrasse 5, 04103 Leipzig, Germany, [‡]Leibniz Institute of Polymer Research Dresden, Hohe Str. 6, 01069 Dresden, Germany, and [§]Department of Physics, Mansoura University, Mansoura 35516, Egypt

Received July 17, 2009; Revised Manuscript Received October 6, 2009

ABSTRACT: Forces of interaction within *single* pairs of poly(2-vinylpyridine) (P2VP) grafted colloids have been measured by optical tweezers (OT) with an extraordinary resolution of ± 0.5 pN. Parameters to be varied are the concentration and type of salt (KCl, CaCl₂, and LaCl₃) of the surrounding medium as well as its pH. The observed force–distance relation is *quantitatively* described by the Jusufi model [*Colloid Polym. Sci.* **2004**, 282, 910–917] for spherical polyelectrolyte brushes which takes into account the entropic effect of the counterions and enables one to estimate the ionic concentration inside the brush. The transition from an osmotic to the salted brush regime is analyzed in detail. For the scaling of the brush height a power law is found having an exponent of 0.24 ± 0.01 , which ranges between the values expected for spherical and planar brushes. At pH 4 a strong transition from a brush to a pancake conformation takes place.

Introduction

Polyelectrolytes are macromolecules whose repeating units bear an electrolyte group. They are used in many applications: for instance, for rheology control, as wet and dry strength additives, as flocculating or dispersing agents, as core–shell particles and hollow capsules for controlled drug delivery.^{1–4} If linear polyelectrolyte chains are grafted densely to planar surfaces, then the result is a planar polyelectrolyte brush while grafting linear polyelectrolyte chains densely to colloidal core latex particles leads to spherical polyelectrolyte brushes in which the curvature of the cores becomes a new decisive length parameter.^{5,6} The conformations of the polymer brushes are affected by a number of factors: the polymer architecture, solvent affinity, grafting density, pH, and the ionic strength of the surrounding medium.⁷

Figure 1 shows the schematic structure of a spherical polyelectrolyte that will form the subject of this article. The core is SiO₂, which is inert and totally impenetrable for the dispersion medium water, and the polyelectrolyte chains are P2VP which are weak cationic polyelectrolyte and pH-responsive polymers. The ratio of the contour length (128 nm) of the P2VP brushes and the radius of the SiO₂ colloids (775 nm) is $\sim 1/6$, a value too high to consider the surfaces as planar but not large enough to treat them as spherical.

The positive charge on the chain in a broad range of pH permits the interaction with negatively charged counterparts. In the present study the counterions are the Cl[−] ions whereas K⁺, Ca²⁺, and La³⁺ are the co-ions. If two spherical polyelectrolyte brushes approach each other, the respective surface layers overlap. Hence, the polymer chains of the two particles start to interact. This leads to steric and electrostatic interactions. The steric interaction is controlled by the geometry and grafting density of the polyelectrolyte chains while the electrostatic

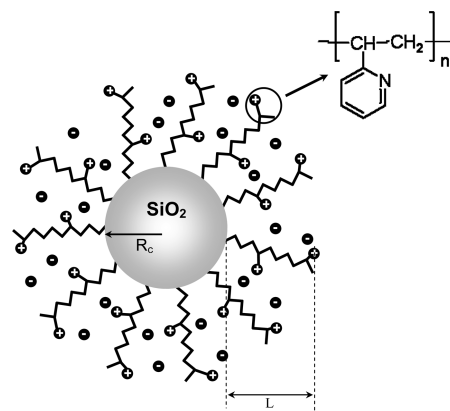


Figure 1. Sketch of the spherical polyelectrolyte brushes investigated. Linear chains of poly(2-vinylpyridine) (P2VP) are densely grafted onto the surface of a colloidal SiO₂ particle by the “grafting to” technique. The radius R_c of the core particle is 1.55 ± 0.04 μm . The thickness L of the P2VP brush on the surface of the particles is determined by the optical tweezers measurements.

interaction is controlled by the charge of the chain and the ionic strength of the medium. The translational entropy of the counterions as well as the elastic entropy of the chain controls the space distribution of the counterions and the conformation of the chain.

For better understanding of the interactions between positively charged P2VP-grafted colloids, it is of great interest to know the interaction forces. Force measurements were carried out using surface force apparatus,^{8–11} AFM colloidal probe technique,^{12,13} and optical tweezers.^{14–20}

Some previous surface force apparatus (SFA) studies of polyelectrolyte brushes have used brushes formed from diblock copolymers.^{21–24} In particular, the force measurements between diblock copolymers of poly(*tert*-butylstyrene) and poly(styrene-sulfonate) (PtBS–PSS) adsorbed on both a hydrophilic surface

*Corresponding author: Tel +49 341 9732551; fax +49 341 9732599; e-mail friedrich.kremer@physik.uni-leipzig.de.

(bare mica) and a hydrophobic surface (modified mica with *N*-octadecyltriethoxysilane (OTE)).²² Surface force experiments and ellipsometric measurements showed that polyelectrolytes tethered to the OTE-modified mica surface are dense enough to form a brush structure, and their behavior can be well described by the scaling brush model, whereas for polyelectrolytes tethered to the bare mica surface, the chains adopted a sparse tethering structure. The effect of salt concentration (C_s) and molecular weight (N) on the height of the self-assembled layers (L_0) was examined in each case. In the low-salt limit, the height of the sparsely tethered chains scales with the degree of polymerization as $L_0 \propto N^{0.7}$. $L_0 N^{-0.7}$ does not depend on the added salt concentration in the low-salt regime and scales with the salt concentration to the -0.17 power in the high-salt regime, in agreement with the scaling prediction for sparsely tethered polyelectrolyte chains.

Schneider et al.²⁵ combined direct SFA measurements of planar brushes with measurement of the rate of slow coagulation²⁶ of the particles in the presence of trivalent lanthanum ions in order to determine the interaction force between two brush layers. The interaction potential was modeled using the force law obtained directly from SFA measurements. This approach was capable of measuring the repulsive interaction down to a strength of 1 kT . The data obtained compared favorably with theoretical values derived from the effective charge of spherical polyelectrolyte brushes.

Optical tweezers²⁷ are experimental tools with extraordinary resolution in determining the relative position ($\pm 3\text{ nm}$) of a microscopic object (diameter $\sim 1\text{ }\mu\text{m}$) “without any mechanical contact” and in measuring the forces acting on it ($\pm 0.5\text{ pN}$). By monitoring the force–distance dependencies between two grafted colloids, it is possible to learn how the concentration and valency of the counterions of the surrounding medium as well as its pH determine the effective interaction between the grafted colloids.

The forces of interaction between DNA-grafted colloids were measured in dependence on the molecular weight, grafting density, and the ion concentration of the surrounding medium.^{18,19} The experimental data were described by a model developed for star polymers close to planar walls²⁸ in which compression of the DNA chains is assumed to be the dominating interaction. Mushroom and brush regimes were observed. The former scaled with the grafting density while the latter showed a transition from an osmotic to a salted brush in good agreement with the scaling law.²⁹

In recent studies using optical tweezers, the forces of interaction within *single* pairs of poly(acrylic acid) (PAA) grafted colloids were measured in dependence on the concentration and valency of the counterions of the surrounding medium as well as its pH.²⁰ The data were *quantitatively* described by the Jusufi model³⁰ for spherical polyelectrolyte brushes which takes into account the entropic effect of the counterions. The transition from an osmotic to salted brush on varying the ionic strength and the valency of the ions of the surrounding medium was observed.

In the present contribution the forces of interaction within *single* pairs of P2VP-grafted colloids are measured using optical tweezers. Parameters to be varied are the concentration, type of salt, and pH of the surrounding medium; the experimental conditions are similar to PAA-grafted colloids; the grafting density and the core size are the same. In addition, the same methodology “grafting to” is used to synthesis the two grafted colloids. The main difference between the two systems is that the P2VP-grafted colloids are positively charged while the PAA-grafted colloids are negatively charged.

Experimental Section

Materials. Monodisperse silica particles with diameter of $1.55\text{ }\mu\text{m}$ and standard deviation of $0.04\text{ }\mu\text{m}$ were purchased in dry

state from Microparticles GmbH (Berlin, Germany). Carboxyl-terminated poly(2-vinylpyridine) (P2VP-COOH, $M_n = 40\,600\text{ g/mol}$, $M_w = 43\,800\text{ g/mol}$), synthesized by anionic polymerization, were purchased from Polymer Source, Inc. Poly(glycidyl methacrylate) (PGMA) ($M_n = 84\,000\text{ g/mol}$) was synthesized by free radical polymerization of glycidyl methacrylate (Aldrich).

Polymer Brushes Synthesis and Characterization. Details of the particle modification and characterization by FTIR-ATR/diffuse reflection IR spectroscopy and thermogravimetric analysis (TGA) are given elsewhere.^{31–33}

Briefly, the “grafting to” approach was used to anchor polymer chains (carboxy-terminated poly(2-vinylpyridine)) onto the surface of silica particles. The synthetic procedure starts with covalent grafting of PGMA onto the particle surface. PGMA was chemisorbed from a 2% chloroform solution. To remove nonadsorbed PGMA, the particles were washed and centrifuged several times in chloroform. For grafting of polymer onto the particle surface, PGMA-coated beads were mixed with a 1 wt % chloroform solution of carboxyl-terminated P2VP-COOH and stirred for 2 h. The solvent was removed by evaporation. The particles were annealed at $150\text{ }^\circ\text{C}$ for 4 h. The ungrafted polymer was removed by multiple circles of redispersing of particles in chloroform and subsequent centrifuging.

FTIR-ATR Spectroscopy. FTIR-ATR spectra were taken with an IFS 55 (Bruker, Germany) spectrometer for all prepared systems.

Diffuse Reflection IR Spectroscopy. was used for determination of the grafted amount of polymer. Details of calibration procedure are given elsewhere.^{31,35} The characteristic bands at $1590/1570\text{ cm}^{-1}$ (for P2VP) were used for the estimation of grafted amount of polymers.

Grafting Density of Polymer (Γ). The distances between grafting sites and thickness of grafted polymer layer (H) were estimated as described elsewhere.³³ The thickness of the polymer layer was 8 nm (dry film) corresponding to a grafting density of 0.12 chains/nm^2 . The distance between grafting sites ($\sim 2.8\text{ nm}$) is smaller than the radius of gyration (R_g) of P2VP polymer coils ($R_g \sim 5\text{ nm}$) in θ -conditions. In a good solvent the polymer chains are swollen, and the $R_g \gg R_{g,\theta\text{-conditions}}$. Consequently, the polymer-grafted film exposed to good solvent can be considered as a brushlike layer.³⁴

Optical Tweezers Setup. For the optical trap an inverted microscope (Axiovert S 100 TV, Carl Zeiss, Jena, Germany) accomplished with a stabilized diode-pumped Nd:YAG laser (1064 nm , 1 W , LCS-DTL 322; Laser 2000, Wessling, Germany) was used. The beam was expanded and coupled into the back aperture of the microscope objective (Plan-Neofluor 100 1.30 Oil, Carl Zeiss, Jena, Germany). Video imaging and the optical position detection were accomplished at 20 frames/s by a digital camera (1M60CL, DALSA, Gröbenzell, Germany). The optical stage was positioned in three dimensions with nanometer resolution using piezoactuators (P-5173CD, Physik Instrumente, Karlsruhe, Germany). The sample cell consisted of a closed chamber that allows the flushing of solutions by a syringe pump. A custom-made micropipet with an inner tip diameter of $0.5\text{ }\mu\text{m}$ was inserted into the chamber to hold one colloid by capillary action. The whole experimental setup was located in a temperature-controlled ($298 \pm 1\text{ K}$) room.

The experiments were performed with one colloid fixed at the tip of a micropipet and the second one in an optical trap, as shown in Figure 2.

The experimental setup of the OT technique is described in more detail by Dominguez et al.²⁰ The approach velocity was $0.25\text{ }\mu\text{m/s}$. The interaction force F is obtained from the displacement of the optical trapped colloid out of its equilibrium position. In other words, optical tweezers force can generally be described by $F = -k_{\text{trap}}\Delta x$, where k_{trap} is the trap stiffness and Δx the displacement of the colloid out of its equilibrium

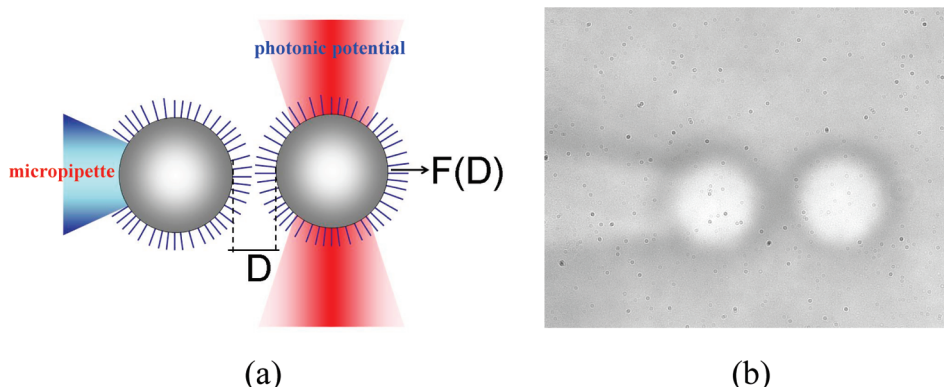


Figure 2. (a) Scheme of the experimental setup of the optical tweezers (OT). One colloid is held with a micropipet by capillary action and the other in the optical trap. The force of interaction F at separation D between the surfaces of the two grafted colloids (diameter of $1.55 \pm 0.04 \mu\text{m}$) is determined from the displacement of the colloid in the optical trap. (b) Microscope image of the two P2VP-grafted colloids in an aqueous medium.

position. From the digital images, the displacement of the colloid in the optical trap out of the equilibrium position (Δx), and the separations between the centers of the colloids were determined using a custom-made LabVIEW image analysis routine.¹⁷ By that the separation between the two colloids could be determined with an accuracy of $\pm 6 \text{ nm}$ and the interacting forces with a resolution of $\pm 0.5 \text{ pN}$. The calibration of the optical trap to determine the trap stiffness (k_{trap}) is based on Stokes law $F = 6\pi\eta rv$, where η is the viscosity of the medium, r the radius of the bead, and v its velocity relative to the surrounding solution.³⁵ A typical force constant for the trap was 0.067 pN/nm . The zero distance between the two grafted colloids is considered as the distance when the hard cores of the grafted colloids touch each other.

Potassium chloride (KCl), calcium chloride (CaCl_2), and lanthanum chloride (LaCl_3) were used as monovalent, divalent, and trivalent salts, respectively. The pH was regulated with HCl and KOH. The conductivity of the solutions was measured with a conductivity probe (EC-CONSEN91W) with built-in temperature sensor (CyberScan PC 510 from EUTECH Instruments) in order to verify the concentration of the solutions. After finalizing the measurements, the reproducibility of the experiment as a whole was ensured by remeasuring the force–separation dependence in the initial salt concentration.

Theory. The theoretical description of uncharged polymer brushes was initiated by de Gennes and Alexander.^{36–38} In

later studies, scaling theories for charged brushes were developed^{29,39–46} taking into account the effects of ionic strength of the surrounding medium, the grafting density, and the molecular weight on the brush height. Furthermore, geometrical effects caused by the curvature of the underlying substrate were taken into account. Pincus²⁹ and Borisov et al.⁴¹ presented scaling theories for charged brushes in the so-called osmotic regime. Inspired by Pincus work and using as starting point a theory developed for star polymers,⁴⁷ Jusufi et al.³⁰ reported a theoretical description of the interactions in spherical brushes. By means of molecular dynamics and mean-field theory, they have demonstrated that the main contribution to the interaction comes from entropic forces associated with the counterions inside the brush. In their approach the following assumptions were made: (i) the two brushes retract and can be modeled as “chopped spheres”, (ii) the dominant term in the potential arises from the entropic contribution of the counterions inside of the brush, and (iii) the electrostatic term is neglected. An effective potential (V_{eff}) for two identical spherical brushes which is function of the colloidal radius (R_c), the separation between the solid surfaces (D), the brush height (L), and the number of counterions inside the brush (Q/e) was obtained.³⁰ The repulsion force between two spherical brushes can be deduced from the derivative of the potential with respect to the position as²⁰

$$F = -\frac{\partial V_{\text{eff}}}{\partial D} = k_B T \left(\frac{Q}{e} \right) \frac{\ln \left(\frac{D+2R_c}{2(L+R_c)} \right) \left(3D+6L+8R_c \ln \left(\frac{R_c}{L+R_c} \right) - 2(D-L+3R_c) \ln \left(\frac{D+2R_c}{2(L+R_c)} \right) \right)}{\left[D+2L-(D+2R_c) \left(\ln \left(\frac{D+2R_c}{2(L+R_c)} \right) \right) \right]^2} \quad (1)$$

where k_B the Boltzmann constant and T the absolute temperature. Taking R_c as fixed and known, it is possible to get from the fits to the experimental data the brush height L and the number of counterions Q/e trapped inside of the brush. From these parameters, the mean counterion concentration inside the brush can be estimated as²⁰

$$C_{\text{brush}} = \frac{Q/e}{N_A \frac{4}{3} \pi ((R_c + L)^3 - R_c^3)} \quad (2)$$

where N_A is the Avogadro number.

Results and Discussion

Optical tweezers enable one to measure the interaction forces between polymer-grafted colloids in the range between 1 and 100 pN without any mechanical contact. To eliminate possible variations between different colloids (variation in the diameter, surface roughness, grafting density, molecular weight, and the charge per colloid, etc.), the experiments are carried out with *single* pairs of colloids for which the solvent is exchanged.

The force–separation dependence as measured within a *single* pair of P2VP-grafted colloids in media of varying KCl concentrations at pH 2 is displayed in Figure 3. At sufficient long separation the force levels to zero, while with decreasing

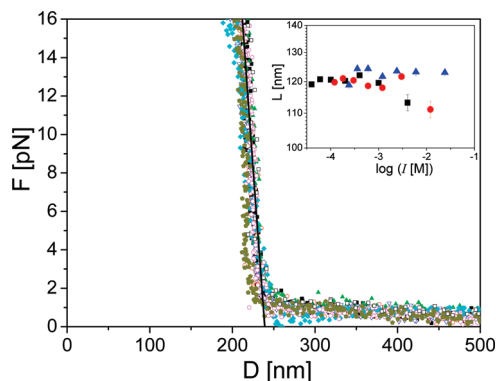


Figure 3. Forces vs separation D as measured for a *single* pair of P2VP-grafted colloids in media of varying KCl concentrations: 4×10^{-5} M (full squares), 6×10^{-5} M (open circles), 10^{-4} M (full up-triangles), 2×10^{-4} M (open down-triangles), 4×10^{-4} M (full diamond), 10^{-3} M (open hexagon), and 4×10^{-3} M (full pentagon) at pH 2. The measurements were made with increasing salt concentrations. At the end of the measurement cycle a 4×10^{-5} M KCl solution was flushed into the sample cell, and it was found that the original force–separation dependence (open squares) is fully recovered. Inset: thickness L of the P2VP brush as a function of the ionic strength I of the KCl (full squares), CaCl_2 (full circles), and LaCl_3 (full up-triangles) salts at pH 2. The solid line represents the fit to 10^{-3} M KCl (full hexagon) concentration using eq 1.

separation the repulsive forces increases monotonously. In order to ensure the experimental reproducibility, at the end of the measurement cycle the sample cell is flushed with the initial concentration (4×10^{-5} M KCl); the force–separation is measured again, and it is found that the original force–separation dependence is recovered.

Interestingly, the salt concentration does not show an effect on the force–separation dependence for the monovalent KCl salt at pH 2. For the identical pair of colloids in media of divalent CaCl_2 and trivalent LaCl_3 ions, the force–separation shows concentration independence as for KCl.

The data can be well described, within experimental uncertainty, by the Jusufi model³⁰ using eq 1. From the fits (the solid line represents the fit to 10^{-3} M KCl as an example) the brush height L (corresponding to half of the separation at an extrapolated acting force of 0 pN) and the number of trapped ions *inside* the brush (Q/e) are obtained. The inset of Figure 3 shows that the brush height L is independent of the ionic strength I as well as the type of salt. A recent work⁴⁸ using zeta potential (ζ -potential) and ellipsometry measurements showed that P2VP brushes are completely dissociated, positively charged, and swollen to more than 10 times its dry thickness at pH < 4 because of a steric repulsion between the brush molecules. At pH 2 the P2VP brushes are fully charged and screened by the counterions condensed within the brush; therefore, the brush height is concentration independent.

In order to gain a deeper understanding of the effect of the pH and ionic strength on the brush height, the force–separation dependence within a *single* pair of P2VP-grafted colloids is measured in varying KCl and CaCl_2 concentrations at pH 4. Figure 4 shows the force–separation dependence as measured within a *single* pair of P2VP-grafted colloids in media of varying KCl concentrations at pH 4. Pronounced effects can be observed. With increasing ionic strength of the surrounding medium the interaction extends to shorter distances at higher ionic strength, reflecting the transition from an osmotic to a salted brush^{18–20} and the concomitant shrinkage of the latter.

The transition from the osmotic to the salted brush takes place when the external salt content equals the counterion concentration inside the brush. The measurements are full reproducible

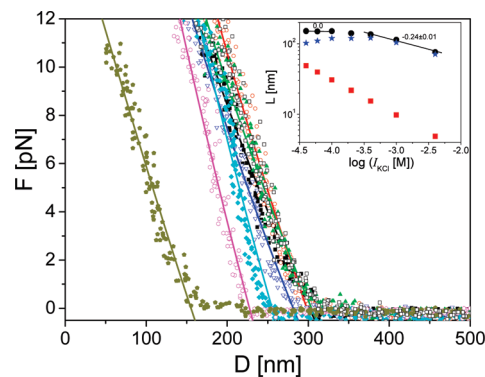


Figure 4. Forces vs separation D as measured for a *single* pair of P2VP-grafted colloids in media of varying KCl concentrations: 4×10^{-5} M (full squares), 6×10^{-5} M (open circles), 10^{-4} M (full up-triangles), 2×10^{-4} M (open down-triangles), 4×10^{-4} M (full diamond), 10^{-3} M (open hexagon), and 4×10^{-3} M (full pentagon) at pH 4. The measurements were made with increasing salt concentrations. In order to ensure the experimental reversibility, at the end of a measurement cycle the force–separation dependence for the initial concentration 4×10^{-5} M KCl was remeasured and proven to coincide within the experimental accuracy (± 0.5 pN) (open squares). The solid lines represent the fits according to eq 1. In the inset the resulting brush height L (full circles), Debye length (full squares), and the nonelectrostatic term calculated as $L - L_{\text{Debye}}$ (full starts) in dependence of the ionic strength I of the KCl are shown. The solid line of slope 0.24 indicates theoretical scaling law predictions for comparison.

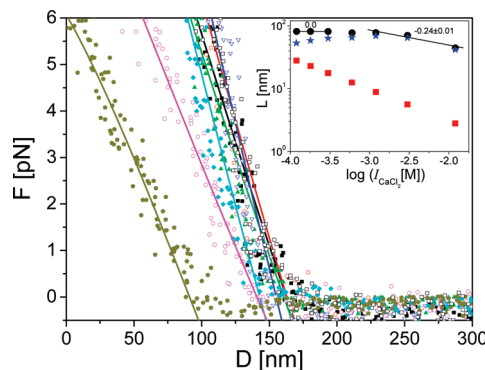


Figure 5. Forces vs separation D as measured for a *single* pair of P2VP-grafted colloids in media of varying CaCl_2 concentrations: 4×10^{-5} M (full squares), 6×10^{-5} M (open circles), 10^{-4} M (full up-triangles), 2×10^{-4} M (open down-triangles), 4×10^{-4} M (full diamond), 10^{-3} M (open hexagon), and 4×10^{-3} M (full pentagon) at pH 4. The measurements were made with increasing salt concentrations. To ensure a full reproducibility of the exchange of the medium and to exclude hysteresis effects due to possible adsorption effects on the colloids, the sample cell was flushed again with 4×10^{-5} M CaCl_2 (open squares). The solid lines represent the fits according to eq 1. In the inset the resulting brush height L (full circles), Debye length (full squares), and the nonelectrostatic term calculated as $L - L_{\text{Debye}}$ (full starts) in dependence of the ionic strength I of the CaCl_2 are shown. The line of slope 0.24 indicates theoretical scaling law predictions for comparison.

after extended periods of time (several hours). From the fits by the Jusufi model using eq 1 (solid lines) the brush height as well as the number of trapped ions inside the brush are obtained. The brush height versus the ionic strength of the surrounding medium (inset of Figure 4) demonstrates the transition from the osmotic regime for KCl concentrations lower than 2×10^{-4} M to the salted regime in which a scaling with a slope of -0.24 ± 0.01 is found. In order to determine the electrostatic contribution to the total repulsion between the colloids the Debye length, L_{Debye} , of the medium is calculated. A maximum for the nonelectrostatic contribution calculated as $L - L_{\text{Debye}}$ is observed at a concentration of the order of 2×10^{-4} M.

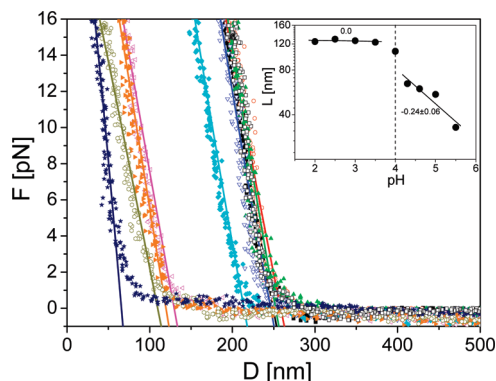


Figure 6. Forces vs separation D as measured for a single pair of P2VP-grafted colloids in media of varying pH: 2 (full squares), 2.5 (open circles), 3 (full up-triangles), 3.5 (open down-triangles), 4 (full diamond), 4.3 (open left-triangles), 4.6 (full right-triangles), 5 (open hexagon), and 5.5 (full stars) at 10^{-3} M KCl. The measurements were done with increasing pH. To ensure full reproducibility of the exchange of the medium, the sample cell was flushed again with 10^{-3} M at pH 2 (open squares) at the end of a measurement cycle. The solid lines represent the fits to the experimental data with eq 1. Inset: brush height L vs pH at 10^{-3} M KCl obtained from analyzing the data using eq 1 (full circles). The line of slope 0.24 indicates theoretical scaling law predictions for comparison.

For the *identical* pair of colloids in media of divalent CaCl_2 ions the forces scale similarly with the separation (Figure 5) as for KCl, but shifted to higher concentrations by 1 order of magnitude. The brush height L in dependence of the ionic strength I in the salted regime again follows a power law with an exponent similar to that of the KCl, 0.24 ± 0.01 . The slope of the brush height versus ionic strength in the salted regime is independent of the type of salt and in good agreement with the scaling law where the slope ranges between $-1/6$ and $-1/3$ as predicted for spherical and planar brushes, respectively.^{29,49,50} Similar results were reported in a previous study, using optical tweezers, by Dominguez et al.²⁰ for PAA-grafted colloids. They found that the brush height scales with an exponent $\sim -1/4$ for both mono- and divalent ions in the salted brush regime.

Figure 6 displays the force–separation dependence for different pH values at a fixed concentration of 10^{-3} M KCl. All curves decay exponentially and the interaction extends to shorter distances with increasing pH values. The Jusufi model describes well (solid lines) the data using eq 1. From the fits the brush height, L , as well as the number of trapped ions inside the brush, Q/e , are obtained as a function of the pH. Surprisingly, the brush height vs the pH (inset of Figure 6) demonstrates a strong transition at pH 4. Two regimes are observed: the first regime ($\text{pH} < 4$) shows that the brush height is nearly independent of the pH while in the second regime ($\text{pH} > 4$) the slope of the brush height versus pH is -0.24 ± 0.06 , similar to the slope of the salted brush in the concentration dependence measurements. Recently, in the same salt concentration (10^{-3} M KCl), the interaction energy between an SiO_2 sphere (diameter $4.77 \mu\text{m}$) and a planar P2VP brush has been measured by Drechsler et al.⁴⁸ at different pH values by using the well-established colloidal probe technique. Although this study has been made on a symmetric system (sphere–plane) which is different from the present system (sphere–sphere), they observed a transition at the same pH 4.

The increase in the brush height of P2VP at $\text{pH} < 4$ is caused by the swelling of the positively charged brush due to the electrostatic repulsions and osmotic pressure between the brush molecules. At $4 < \text{pH} < 6$, the repulsive force becomes weaker and the brush collapse to its dry thickness forming a “pancake”-like conformation. At $\text{pH} > 6$ (the isoelectric point (IEP), i.e., the pH value at which the ζ -potential changes its sign, is for P2VP at

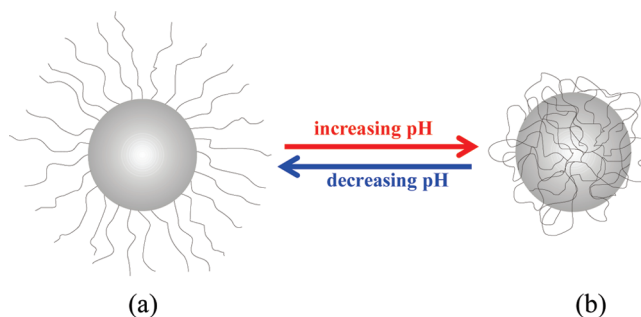


Figure 7. Schematic illustration of the P2VP conformations with increasing and decreasing pH values. (a) At $\text{pH} < 4$ the P2VP chains are stretched away from the surface, forming a brush-like conformation. (b) At $\text{pH} > 4$ the P2VP segments adsorb strongly to the underlying surface in a “pancake”-like conformation.

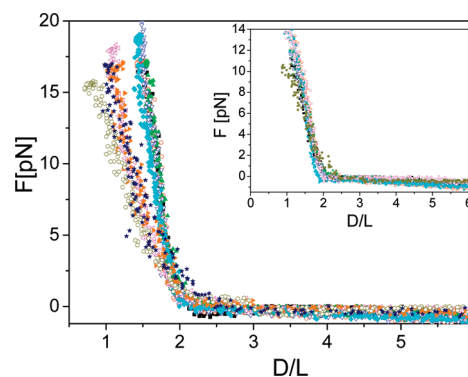


Figure 8. Forces vs normalized separation D/L as measured for a single pair of P2VP-grafted colloids in media of varying pH: 2 (full squares), 2.5 (open circles), 3 (full up-triangles), 3.5 (open down-triangles), 4 (full diamond), 4.3 (open left-triangles), 4.6 (full right-triangles), 5 (open hexagon), and 5.5 (full stars) at 10^{-3} M KCl. Inset: the force vs normalized separation as measured for a single pair of P2VP-grafted colloids in media of varying KCl concentrations: 4×10^{-5} M (full squares), 6×10^{-5} M (open circles), 10^{-4} M (full up-triangles), 2×10^{-4} M (open down-triangles), 4×10^{-4} M (full diamond), 10^{-3} M (open hexagon), and 4×10^{-3} M (full pentagon) at pH 4.

pH 6.7), the steric repulsion disappears and an attractive force becomes visible. The transformation from the brush-like to pancake-like conformation of the P2VP brushes with in dependence on pH is illustrated in Figure 7.

The negative ζ -potential of P2VP above the isoelectric point is caused by the adsorption of OH^- ions on a primarily uncharged surface.⁴⁸ In contrast to ref 20 with PAA-grafted colloids having the same grafting density (~ 0.1 chain/ nm^2), it is observed that the brush height increases with pH due to the electrostatic repulsion and osmotic pressure between the brush molecules. The main difference between the two systems is that the P2VP-grafted colloids are positively charged (IEP at pH 6.8) while PAA-grafted colloids are negatively charged (IEP at pH 2.6). The similarities include that both are weak polyelectrolytes (acid dissociation constant $\text{p}K_a$ for PAA ~ 4.7 while $\text{p}K_a$ for P2VP ~ 2.3) having almost the same grafting density (~ 0.1 chains/ nm^2), molecular weight, and core size ($1.55 \pm 0.04 \mu\text{m}$).

In order to separate the effects of ion concentration and pH, the forces are represented as a function of the reduced distance (D/L) for varying pH at a fixed ion concentration (Figure 8) and vice versa. For the former case it is *not* possible to obtain a “master curve” in contrast to the latter (inset of Figure 8). The reason might be the different brush charges that lead to different Q values in eq 1.

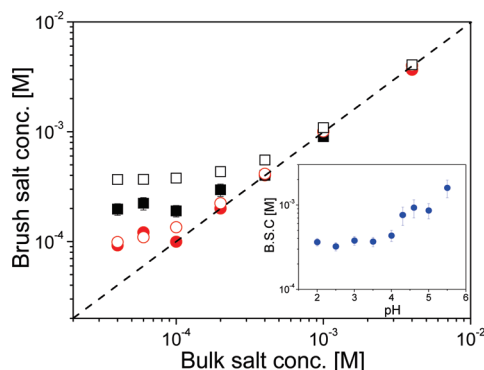


Figure 9. Salt concentration inside the brush (“brush salt concentration”) vs the salt concentration in the bulk of KCl (full circles) and CaCl_2 (full squares) at pH 4 calculated from eq 2 (Jusufi approach). The dashed line indicates the equality of the salt concentration inside and outside the brush. Open symbols represent the salt concentration according to eq 3 (Hariharan approach) for KCl (open circles) and CaCl_2 (open squares). Inset: brush salt concentration (BSC) for 10^{-3} M KCl at varying pH.

As mentioned above, from the fits by the Jusufi model using eq 1, the number of counterions trapped inside the brush Q/e is obtained and can be used to determine the ion concentration inside the brush using eq 2.

The comparison for the monovalent KCl and the divalent CaCl_2 salts at pH 4 shows (Figure 9) the extent to which it is higher than the ion concentration in the surrounding medium, especially in the osmotic regime where the counterions are trapped inside the brush. It is important to mention that the model (eq 1) assumes that only a small fraction of charges is outside the brush, so the electrostatic repulsion is much smaller than the entropic effect. This assumption is not fulfilled for salt concentrations lower than 2×10^{-4} M, with increasing ionic strength the concentration inside and outside of the brush tends to equalize. The pH dependence of the salt concentration inside the brush shows two regimes (inset of Figure 9). In the first regime where the $\text{pH} < 4$, the salt concentration inside the brushes (BSC) is pH independent, while in the second regime where $\text{pH} > 4$, the BSC increases with increasing pH. This tendency is opposite to the reported results of the PAA-grafted colloids²⁰ where the BSC decreases with increasing the pH.

Hariharan et al.⁵¹ developed a theory for strongly curved surfaces. In this theory the “effective” ionic strength in the brush, c_{brush} , is related to the added salt concentration c_a by^{20,52}

$$c_{\text{brush}} = \frac{1}{2} \sum_i \frac{n_i z_i^2}{N_A} = c_a \left[1 + \left(\frac{z \rho_f}{2e N_A c_a} \right)^2 \right]^{1/2} \quad (3)$$

where c_{brush} and c_a are the salt concentration inside the brush and in the bulk, n_i is the number density of the ions of species i , z_i is the valence of the ions, N_A the Avogadro number, e the electron charge, and ρ_f the average charge density defined as

$$\rho_f = - \sum_i e z_i n_i = \frac{3e R_c^2 \sigma L_c}{l_c [(R_c + L)^3 - R_c^3]} \quad (4)$$

where σ is the grafting density, R_c the colloid radius, L_c the contour length, and l_c the distance between the charges. The distance between the charges (l_c) is the Bjerrum length ($= 0.714$ nm in H_2O at 25°C). The Bjerrum length is the distance at which the unscreened Coulomb interaction energy of a pair of monovalent ions equals $k_B T$.

As shown in Figure 9, a discrepancy can be observed between the values calculated using the Hariharan and the Jusufi approaches at low salt concentration, and starting from 2×10^{-4} M good agreement between both is found. It should be noted that in the Jusufi model electrostatic repulsion is neglected, which does not hold at low concentrations. On the other hand, eq 3 is valid for highly curved surfaces a condition not fulfilled in our experiments.

Conclusions

The forces of interaction within *single* pairs of the P2VP-grafted colloids have been measured by optical tweezers. Parameters varied are the concentration, the type of salt of the surrounding medium, and the pH. The Jusufi model³⁰ is used to describe the force–separation curves. From the fitting using this model the brush height as well as the number of counterions inside the brush is deduced as a function of the ionic strength and pH. At pH 2, the brush height is independent of the ionic strength as well as the type of salt. The brush height versus the ionic strength of the surrounding medium demonstrates the transition from an osmotic to salted brush at pH 4. Power law dependence with an exponent of -0.24 is found for both mono- and divalent ions in the salted brush regime. This value ranges between those predicted for spherical and planar brushes which are reasonable due to the geometrical conditions. Increasing the pH results in the transformation from the brush-like to pancake-like conformation of the P2VP brushes. The Hariharan et al. model⁵¹ for strongly curved surfaces compares well with the results of the Jusufi approach.

The comparison between the P2VP-grafted colloids with the recent published results of the PAA-grafted colloids²⁰ reveal similarities but also some distinct differences. The similarities include (i) the interaction is dominated by entropic forces resulting from the counterion distribution inside the brush and can be estimated by means of the Jusufi approach, (ii) transition from an osmotic to a salted brush on varying the ionic strength of the surrounding medium, and (iii) the brush height in dependence of the ionic strength in the salted regime scales with an exponent of ~ 0.25 . The main difference is the pH dependence of both systems. For the PAA-grafted colloids, the brush height increases with increasing pH while the P2VP-grafted colloids show a transformation in the conformation of the brushes.

Acknowledgment. The authors thank Dr. Gustavo Dominguez-Espinosa for his comments. Support by the Deutsche Forschungsgemeinschaft (DFG) for financial support within the project “In situ investigation of interaction forces of polyelectrolyte brushes” and Project SY125/1-1 is gratefully acknowledged.

References and Notes

- (1) Tripathy, S. K.; Kumar, J.; Nalwa, H. S. *Handbook of Polyelectrolytes and Their Applications*; American Scientific Publications: Stevenson Ranch, 2002; Vols. 1–3.
- (2) Rosoff, M. *Nano-Surface Chemistry*; Marcel Dekker, Inc.: New York, 2001.
- (3) Evans, D. F.; Wennerström, H. *The Colloidal Domain Where Physics, Chemistry, Biology, and Technology Meet*; 2nd ed.; VCH: New York, 1999.
- (4) Radeva, T. *Physical Chemistry of Polyelectrolytes*; Marcel Dekker, Inc.: New York, 2001; Vol 99.
- (5) Advincula, R. C.; Brittain, W. J.; Caster, K. C.; Rühle, J. *Polymer Brushes*; Wiley-VCH: Berlin, 2004.
- (6) Guo, X.; Weiss, A.; Ballauff, M. *Macromolecules* **1999**, *32*, 6043–6046.
- (7) Claesson, P. M.; Poptoshev, E.; Blomberg, E.; Dedinaite, A. *Adv. Colloid Interface Sci.* **2005**, *114*, 173–187.

- (8) Klein, J.; Kumacheva, E.; Perahia, D.; Mahalu, D.; Warburg, S. *Faraday Discuss.* **1994**, 98, 173–188.
- (9) Balastre, M.; Li, F.; Schorr, P.; Yang, J.; Mays, J. W.; Tirrell, M. V. *Macromolecules* **2002**, 35, 9480–9486.
- (10) Sheth, S. R.; Efremova, N.; Leckband, D. E. *J. Phys. Chem. B* **2000**, 104, 7652–7662.
- (11) Dunlop, I. E.; Briscoe, W. H.; Titmuss, S.; Jacobs, R. M. J.; Osborne, V. L.; Edmondson, S.; Huck, W. T. S.; Klein, J. *J. Phys. Chem. B* **2009**, 113, 3947–3956.
- (12) Limpoco, F. T.; Advincula, R. C.; Perry, S. S. *Langmuir* **2007**, 23, 12196–12201.
- (13) Vyas, M. K.; Schneider, K.; Nandan, B.; Stamm, M. *Soft Matter* **2008**, 4, 1024–1032.
- (14) Salomo, M.; Kegler, K.; Gutsche, C.; Reinmuth, J.; Skokow, W.; Kremer, F.; Hahn, U.; Struhalla, M. *Colloid Polym. Sci.* **2006**, 284, 1325–1331.
- (15) Salomo, M.; Kroy, K.; Kegler, K.; Gutsche, C.; Struhalla, M.; Reinmuth, J.; Skokow, W.; Immische, C.; Hahn, U.; Kremer, F. *J. Mol. Biol.* **2006**, 359, 769–776.
- (16) Gutsche, C.; Salomo, M.; Kim, Y. W.; Netz, R. R.; Kremer, F. *Microfluid. Nanofluid.* **2006**, 2, 381–386.
- (17) Gutsche, C.; Keyser, U. F.; Kegler, K.; Kremer, F.; Linse, P. *Phys. Rev. E* **2007**, 76, 031403–031409.
- (18) Kegler, K.; Salomo, M.; Kremer, F. *Phys. Rev. Lett.* **2007**, 98, 058304–058307.
- (19) Kegler, K.; Konieczny, M.; Dominguez-Espinosa, G.; Gutsche, C.; Salomo, M.; Kremer, F.; Likos, C. N. *Phys. Rev. Lett.* **2008**, 100, 118302–118305.
- (20) Dominguez-Espinosa, G.; Synytska, A.; Drechsler, A.; Gutsche, C.; Kegler, K.; Uhlmann, P.; Stamm, M.; Kremer, F. *Polymer* **2008**, 49, 4802–4807.
- (21) Raviv, U.; Giasson, S.; Kampf, N.; Gohy, J. F.; Jerome, R.; Klein, J. *Nature* **2003**, 425, 163–165.
- (22) Li, F.; Balastre, M.; Schorr, P.; Argillier, J. F.; Yang, J.; Mays, J. W.; Tirrell, M. *Langmuir* **2006**, 22, 4084–4091.
- (23) Kampf, N.; Gohy, J. F.; Jerome, R.; Klein, J. *J. Polym. Sci., Part B: Polym. Phys.* **2005**, 43, 193–204.
- (24) Raviv, U.; Giasson, S.; Kampf, N.; Gohy, J. F.; Jerome, R.; Klein, J. *Langmuir* **2008**, 24, 8678–8687.
- (25) Schneider, C.; Jusufi, A.; Farina, R.; Li, F.; Pincus, P.; Tirrell, M.; Ballauff, M. *Langmuir* **2008**, 24, 10612–10615.
- (26) Holthoff, H.; Egelhaaf, S. U.; Borkovec, M.; Schurtenberger, P.; Stricher, H. *Langmuir* **1996**, 12, 5541–5549.
- (27) Ashkin, A. *Phys. Rev. Lett.* **1970**, 24, 156–159.
- (28) Konieczny, M.; Likos, C. N. *J. Chem. Phys.* **2006**, 124, 214904–214915.
- (29) Pincus, P. *Macromolecules* **1991**, 24, 2912–2919.
- (30) Jusufi, A.; Likos, C. N.; Ballauff, M. *Colloid Polym. Sci.* **2004**, 282, 910–917.
- (31) Synytska, A.; Ionov, L.; Dutschk, V.; Minko, S.; Eichhorn, K.-J.; Stamm, M.; Grundke, K. *Prog. Colloid Polym. Sci.* **2006**, 132, 72–81.
- (32) Synytska, A.; Ionov, L.; Dutschk, V.; Stamm, M.; Grundke, K. *Langmuir* **2008**, 24, 11895–11901.
- (33) Berger, S.; Synytska, A.; Ionov, L.; Eichhorn, K.-J.; Stamm, M. *Macromolecules* **2008**, 41, 9669–9676.
- (34) Ionov, L.; Sidorenko, A.; Eichhorn, K. J.; Stamm, M.; Minko, S.; Hinrichs, K. *Langmuir* **2005**, 21, 8711–8716.
- (35) Svoboda, K.; Block, S. M. *Annu. Rev. Biophys. Biomol. Struct.* **1994**, 23, 247–285.
- (36) de Gennes, P. G. *J. Phys. (Paris)* **1976**, 37, 1445–1452.
- (37) de Gennes, P. G. *Macromolecules* **1980**, 13, 1069–1075.
- (38) Alexander, S. *J. Phys. (Paris)* **1977**, 38, 977–981.
- (39) Zhulina, E. B.; Birshtein, T. M.; Borisov, O. V. *Macromolecules* **1995**, 28, 1491–1499.
- (40) Milner, S. T. *Science* **1991**, 251, 905–914.
- (41) Borisov, O. V.; Birshtein, T. M.; Zhulina, E. B. *J. Phys. II* **1991**, 1, 521–526.
- (42) Ross, R. S.; Pincus, P. *Macromolecules* **1992**, 25, 2177–2183.
- (43) Zhulina, E. B.; Borisov, O. V.; Birshtein, T. M. *J. Phys. II* **1992**, 2, 63–74.
- (44) Borisov, O. V.; Zhulina, E. B.; Birshtein, T. M. *Macromolecules* **1994**, 27, 4795–4803.
- (45) Zhulina, E. B.; Borisov, O. V. *J. Chem. Phys.* **1997**, 107, 5952–5967.
- (46) Naji, A.; Seidel, C.; Netz, R. R. *Adv. Polym. Sci.* **2006**, 198, 149–183.
- (47) Jusufi, A.; Likos, C. N.; Löwen, H. *J. Chem. Phys.* **2002**, 116, 11011–11027.
- (48) Drechsler, A.; Synytska, A.; Uhlmann, P.; Stamm, M.; Kremer, F. Manuscript in preparation.
- (49) Biesalski, M.; Rühle, J.; Johannsmann, D. *J. Chem. Phys.* **1999**, 111, 7029–7037.
- (50) Daoud, M.; Cotton, J. P. *J. Phys. (Paris)* **1982**, 43, 531–538.
- (51) Hariharan, R.; Biver, C.; Russel, W. B. *Macromolecules* **1998**, 31, 7514–7518.
- (52) Guo, X.; Ballauff, M. *Langmuir* **2000**, 16, 8719–8726.